MEMS actuated wavelength drop filter based on microsphere whispering gallery modes

Robert Blue, Li Li, Gordon M H Flockhart, and Deepak Uttamchandani

Centre for Microsystems and Photonics, Department of Electronic and Electrical Engineering, University of Strathclyde, 204 George Street, Glasgow G1 1XW, UK

Email: gordon.flockhart@eee.strath.ac.uk

Abstract

MEMS enabled tuneable optical coupling between optical microsphere resonators and optical fibre waveguides is reported. We describe the design, fabrication and experimental characterisation of a MEMS platform, based on electrothermal actuators, which controls the resonator-to-waveguide separation. We compare the simulated and experimental displacements of the actuators in an unloaded and loaded state, where the load is a 1 mm optical spherical resonator. We then demonstrate the proof of concept application of selective wavelength dropping using the MEMS platform by modulating the coupling between the spherical resonator and a tapered optical fibre waveguide.

PACS Codes: 85.85.+j, 42.82.Fv, 42.79.Sz

1. Introduction

Synchronous optical coupling between optical waveguides and optical resonant structures has been used in many optical communication devices such as compact add/drop filters [1,2], low-power wavelength-tuneable modulators [3], low-threshold Raman lasers [4], and also in ultrasensitive label-free biosensing [5,6]. There are two general approaches used for optical waveguide-to-resonator coupling. The first is based on integrated optics (IO) where the optical waveguide is an integrated optical channel waveguide, while the resonant structure is an integrated optic ring resonator [2], or an integrated optic disc resonator [7]. The second approach uses modified single mode optical fibre waveguides, either side-polished optical fibre half couplers [8], angle polished optical fibres [9], adiabatically tapered single mode fibres [10,11], or bent optical fibres [12], while optical spheres fabricated from transparent optical materials, such as silica, serve as the optical resonators supporting whispering gallery modes [13]. Based on this optical fibre-to-spherical resonator coupling, a proof of concept optical communication device has been reported [1,14]. For example, Cai et al. [1] demonstrated a static (fixed) four port add-drop device based on two optical fibre taper sections in physical contact with a 300 μm diameter silica microsphere. Successful wavelength selective channel exchange between the two fibres on opposite sides of the microsphere was achieved with an insertion loss of 3 dB by coupling to an optical whispering gallery mode of the microsphere. Bilici et al. [14] utilised a 1 mm sphere of BK7 glass to demonstrate a dropping filter coupling 0.5 dB to a photodiode.

This manuscript is the peer-reviewed, accepted author manuscript of the following article: Blue, R., Li, L., Flockhart, G., & Uttamchandani, D. (2011). MEMS-actuated wavelength drop filter based on microsphere whispering gallery modes. Journal of Micromechanics and Microengineering, 21(11), [115020]. 10.1088/0960-1317/21/11/115020

When either the IO based approach or the fibre optics based approach is followed, the optical coupling strength of the waveguide and resonator remains fixed (assuming constant temperature conditions) and is determined by the physical separation and mode mismatch between waveguide and resonator. Recently, it has been demonstrated that the coupling between an IO waveguide and IO resonator can be made tuneable, or variable, by incorporating micro-electro-mechanical systems (MEMS) actuators into the device design. The MEMS microactuators can very precisely control the physical separation between the IO waveguide and IO resonator, thereby modulating the optical transmission through the waveguides. This experimentally demonstrated concept has produced tuneable IO devices such as a waveguide and microdisk integrated on a silicon-on-insulator (SOI) substrate [15]. Using the MEMS actuation, the waveguide deforms and changes the gap spacing between the waveguide and disk to attenuate the waveguide transmittance by up to 30 dB. Similarly an electrostatic comb-drive micro-actuator has been connected to a silicon microring resonator to create a wavelength-selective add-drop switch [16]. By applying voltages from 0 V to 28 V, the actuator adjusted the coupling efficiency between the microring and the waveguides and the transmission was varied by up to 33 dB. The full-width-half-maximum bandwidth of the dropped wavelength was 0.5 nm, corresponding to an optical quality-factor, Q-value, of over 3000.

In terms of a system incorporating a tapered optical fibre and an optical microsphere resonator, no equivalent compact MEMS based arrangement for accurate physical separation control between the tapered optical fibre and optical microsphere, to vary the optical coupling, has been demonstrated. Optical fibre waveguides are used extensively throughout optical communication systems and losses in these systems are primarily due to intrinsic and extrinsic absorption, scattering and connection losses. The optical fibre-to-spherical resonator architecture has the potential advantage of lower insertion loss compared to IO devices as it obviates the need to couple the propagating light to an IO waveguide structure. This connection typically results in coupling loss due to misalignment and mode mismatch, i.e. mode-field diameter. Coupling from tapered optical fibres to silica optical microspheres with high Q-factors ($>10^8$) has been reported to achieve near lossless coupling with transmission > 99% [17]. Optical microspheres can also achieve higher Q-factors when compared to integrated optic rings and disks. In the case of optical fibre coupling to silica microspheres, Q-factors as high as 10^8 to 10^{10} have been reported [18], which are several orders of magnitude higher than integrated optical resonators, with resultant resonant optical linewidths less than 1 MHz. Narrow linewidth filters are of interest for applications such as single frequency operation of fibre lasers and high sensitivity sensing applications [19].

In this paper we report a compact architecture which addresses the unsolved issue of providing variable coupling between an optical fibre and a spherical optical resonator. This has been achieved by using a MEMS-based solution. We have fabricated an electrothermally actuated MEMS platform on which a spherical optical resonator is supported. Adjacent to the surface of the sphere a tapered section of an unbroken optical fibre is positioned. By actuation of the compact MEMS platform, the separation between the fibre taper and sphere can be precisely varied in a repeatable way, thereby controlling the evanescent optical coupling between the two optical structures. Through this process, the optical transmission spectrum of the fibre waveguide is modified.

The remainder of this paper is divided as follows: in section 2 we briefly describe the phenomenon of whispering gallery modes (WGMs) that exist in spherical resonators. In section 3 we provide details of the silicon MEMS platform. In section 4 we present some experimentally measured characteristics of the platform. In section 5 we present some simulation results of the platform behaviour with comparisons made to the experimental measurements. In section 6 and 7 we provide details of the optical experiments conducted to demonstrate an application of the platform to in-line channel dropping. Finally, sections 8 and 9 discuss the findings of the work and conclude the paper respectively.

2. Background

This manuscript is the peer-reviewed, accepted author manuscript of the following article: Blue, R., Li, L., Flockhart, G., & Uttamchandani, D. (2011). MEMS-actuated wavelength drop filter based on microsphere whispering gallery modes. Journal of Micromechanics and Microengineering, 21(11), [115020]. 10.1088/0960-1317/21/11/115020

Within a spherical optical resonator a so-called whispering gallery mode can occur when light strikes the interior interface with an angle greater than the critical angle of the sphere and is totally internally reflected back into the sphere to undergo further reflections [19]. Thus the electromagnetic energy is trapped within the sphere and propagates by total internal reflection around the circumference of the sphere. If, after each circumnavigation of the sphere, the guided light arrives at its starting point in phase with the light being coupled to the sphere, then constructive interference will occur and a resonance is established. This resonance will only occur for discrete optical wavelengths dependent on the refractive index and dimensions of the sphere. Using this simplified view of a circumferential resonant mode, the free spectral range, $\Delta\nu_{FSR}$, of this spherical resonator is given by

$$\Delta\nu_{FSR} \approx \frac{c}{2\pi an} \quad (1)$$

where c is the speed of light, $2a$ is the diameter of the sphere, and n is its refractive index.

The spherical optical resonator can support a variety of optical modes, denoted by three mode numbers which represent the radial, equatorial and polar components and are morphology dependent [19]. The radial mode number is equal to the number of field maxima in the equatorial plane. A radial mode includes an evanescent field component that decays exponentially beyond the interface. This diverse range of modes has been exploited, for example, to control the power transfer in narrow-band wavelength-filtering devices [20].

A WGM can be established in a spherical resonator by phase matched evanescent field coupling [10] via frustrated total internal reflection to the resonator mode by overlapping the evanescent field of the spherical resonator with the evanescent field of a nearby external optical waveguide. The coupling of the evanescent fields between the tapered fibre and microsphere is dependent on the separation of the two and this is typically adjusted to achieve optimum coupling and the separation is in the order of 0 - 2 μm [17,21].

3. Description and fabrication of MEMS platform

Different types of MEMS actuators have been reported [22] and the forces generated from certain actuators have been calculated [23]. Electrothermal actuators are widely used in MEMS devices and are capable of generating large forces [24]. A MEMS electrothermally actuated platform was designed with the objective of accurately and repeatedly lifting a 1 mm diameter sphere which serves as a spherical optical resonator.

An electron micrograph of the MEMS platform used in our work is shown in figure 1**Error! Reference source not found.**. The platform has an array of 8 identical electrothermal microactuators in a symmetric radial format; the actuators are electrically connected in series during experiments. The radial actuator arrangement allows the spherical resonator to be positioned in the octagonal gap which is formed at the centre. This gap has a size of 800 μm, which allows the 1 mm diameter spherical resonator to sit at the centre. Each actuator has two “hot” arms and two “cold” arms. The simulated temperature distribution and displacement during actuation for this type of out-of-plane actuator has been obtained and will be presented in section 5. The out-of-plane movement of the thermally actuated MEMS platform originates from the combined effect of the initial stress gradient through the SOI structural layer and the thermal expansion forces produced from the Joule heating. The stress gradient is a well known feature of the SOIMUMPs fabrication process used to fabricate our platform [25]. The source of the stress gradient is due to a combination of effects arising from the non-uniform dopant distribution through the thickness of the silicon and the wafer polishing process to achieve the desired thickness [26]. The residual stress gradient generates an inherent out-of-plane curvature of the cantilever-like suspended thermal actuators with no applied power. When a DC current is passed through the two inner beams of the thermal actuator, the Joule heating causes the two inner beams to try to expand along their length while the two outer beams are at a lower temperature because they do not carry a current, and therefore do not expand as much as the inner beams. The net effect of the forces produced by the differential expansion is a further “vertical” displacement from the initial vertical out-of-plane displacement arising from the stress gradient.

This manuscript is the peer-reviewed, accepted author manuscript of the following article: Blue, R., Li, L., Flockhart, G., & Uttamchandani, D. (2011). MEMS-actuated wavelength drop filter based on microsphere whispering gallery modes. Journal of Micromechanics and Microengineering, 21(11), [115020]. 10.1088/0960-1317/21/11/115020

In our design each electrothermal actuator was 1800 μm long from the anchor to the tip of the free-end. The connection beam at the free-end was 290 μm long and 40 μm wide. The inner two beams have widths of 30 μm while the outer two beams have widths of 40 μm. The eight thermal actuators are patterned in the top single crystal silicon structural layer of 10 μm thickness. The tips of the eight thermal actuators were measured to have an average initial out-of-plane displacement of 5.4 μm.

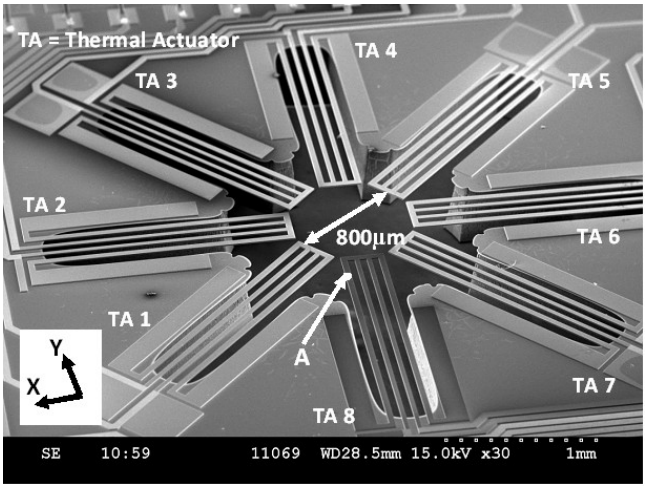

Figure 1. Electron micrograph of electrothermal actuated MEMS platform showing the 8 beams that displace upwards when current is applied, point A is located 100 μm away from the tip.

4. Experimental characterisation of the MEMS platform

The average electrical resistance of the thermal actuators at room temperature was measured to be 2.54 kΩ with a standard deviation of 0.027 kΩ. The maximum applied voltage to each thermal actuator was 25 V for individual testing. The function of the platform requires only a relatively small vertical displacement compared to its maximum achievable displacement. Therefore, the MEMS platform was typically characterized at less than 12 V per thermal actuator.

The static mode (or DC) vertical displacement of the MEMS platform was measured by using an optical surface profiler (NT1100, Veeco). The eight thermal actuators were connected in series to have the same current. The driving DC voltage from 0 V to 90 V in steps of 5 V was supplied to the MEMS platform. At each voltage value the surface profile of the entire device was recorded. From this data, the vertical displacement of the four beams in each thermal actuator were measured approximately 100 μm from the tip of the actuator, as indicated by point A in figure 1. Initially an unloaded MEMS platform was measured by following this method and the results are shown in figure 3, where each point is the average displacement of all four beams in all eight thermal actuators at the same electrical current; the measurement variation is presented using the error bars to plot the standard deviation. The beam displacements were observed to vary slightly at the same DC drive power. The source of these variations is not precisely known

This manuscript is the peer-reviewed, accepted author manuscript of the following article: Blue, R., Li, L., Flockhart, G., & Uttamchandani, D. (2011). MEMS-actuated wavelength drop filter based on microsphere whispering gallery modes. Journal of Micromechanics and Microengineering, 21(11), [115020]. 10.1088/0960-1317/21/11/115020

and may be due to the slight difference of the resistances of each actuator and the mechanical material properties between the eight thermal actuators, e.g. due to anisotropic Young's modulus of single crystal silicon. Also, local variations in the boundary conditions between the electrothermal actuator, the optical sphere and the surrounding air layer may also contribute to the observed differences between the actuators.

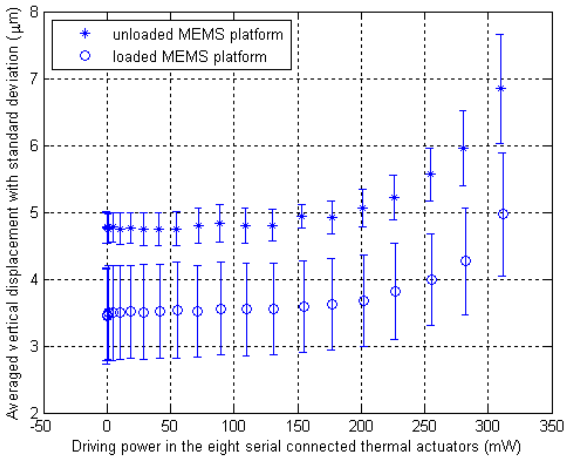

Figure 2. Averaged vertical displacement, at point A, of eight thermal actuators where the error bars denote the standard deviation for an unloaded (o) and loaded case (*).

Subsequently, an optical sphere with a diameter of 1 mm and a mass of 1.4 mg was freely placed in the centre of the same MEMS platform, and the characterisation was repeated using the same method. The diameter of the sphere is larger than the octagonal hole in the centre of the platform; therefore when the sphere was loaded on to the MEMS actuators, the optical surface profiler's view of the actuator tips was obscured. As described previously, the displacement measurements were performed 100 μm from the actuator tip to allow direct comparisons to be made with the measured displacements of the unloaded case. The measured displacements for the loaded case with a free sitting sphere are shown in figure 2. The unloaded and loaded (free sitting sphere) measurements show that this type of thermal actuator exhibits a threshold effect and, as would be expected, the effect of loading the actuator with the sphere reduces the deflection for the same driving power. Also, a larger displacement variation of the eight thermal actuators was seen to occur at higher driving power for the unloaded platform. Possible reasons for this include: variations of resistance in each actuator; potential anisotropic stress distributions in the actuators after fabrication; and the anisotropic elastic property of the structural silicon layer. When the large force (in μN range) is loaded onto, or generated in the thermal actuators, the difference of Young's modulus will result in a displacement variation between the thermal actuators. A comparison of vertical displacements between two adjacent thermal actuators in the platform will be described in section 5.

5. Simulation of the MEMS platform

The electro-thermo-mechanical behaviour of the thermal actuators has been simulated by the finite element analysis software - CoventorWare (Coventor, Inc.). The material properties used in the device model are applied using the SOIMUMPS material database (listed in Table 1) incorporated within CoventorWare. Specific material properties like the electrical conductivity and the stress gradient are experimentally measured by electrical and curvature measurements of one of the actuators on the platform. The gravitational loading force of the 1 mm sphere was assumed to be equally distributed between the eight thermal actuators, and applied to their tip. Figure 3(a) and (b) show the electro-thermo-mechanical

This manuscript is the peer-reviewed, accepted author manuscript of the following article: Blue, R., Li, L., Flockhart, G., & Uttamchandani, D. (2011). MEMS-actuated wavelength drop filter based on microsphere whispering gallery modes. Journal of Micromechanics and Microengineering, 21(11), [115020]. 10.1088/0960-1317/21/11/115020

simulation for the temperature distribution and vertical displacement respectively, generated using the CoventorWare simulation tool.

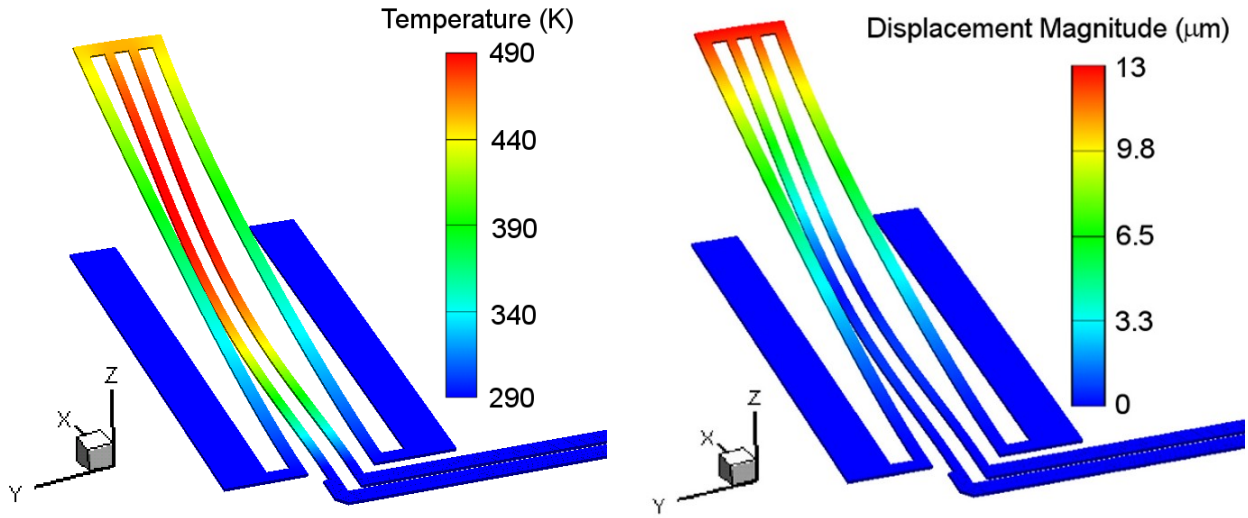

Figure 3. The simulated (a) temperature (°K) and (b) vertical displacement (μm) distribution of the unloaded thermal actuator (TA 6 in figure 1) at 45.4 mW.

The vertical displacement of the thermal actuators numbers five and six, TA 5 and TA 6 in figure 1, was calculated and compared to the experimental measurements in the cases where the device was unloaded and loaded with a free sitting sphere, see fFigure and Figure respectively. For both simulation and experimental characterisation, the vertical displacements of TA 5 and 6 are measured at points 100 μm away from the thermal actuator tip (point A in figure 1) for both unloaded and microsphere loaded cases. At the maximum driving power, the vertical displacements of the loaded MEMS thermal actuator are about 2 μm lower than the values for the unloaded thermal actuator in both simulation and experiment. Figures 4 and 5 show good agreement between the actuator's threshold behaviour in the simulation and experimental results. The difference between the two sets of results at higher driving power is thought to be due to the assumption of constant electrical and mechanical material properties of the SOI layer during the simulation. The electric conductivity of the doped silicon is a temperature dependent value and is dependent on the doping level; however this is not specified for the SOIMUMPs fabrication process, hence we have used a constant value of electric conductivity of 5.56 mS μm^{-1}. Also, the Young's modulus decreases with increasing temperature [27].

This manuscript is the peer-reviewed, accepted author manuscript of the following article: Blue, R., Li, L., Flockhart, G., & Uttamchandani, D. (2011). MEMS-actuated wavelength drop filter based on microsphere whispering gallery modes. Journal of Micromechanics and Microengineering, 21(11), [115020]. 10.1088/0960-1317/21/11/115020

Table 1. Material properties of silicon-on-insulator used in the simulation.

Material Properties	Value	
Material	SOI	BK7 Glass
Young's Modulus (TA 1, 3, 5,7)	130 GPa	81 GPa
Young's Modulus (TA 2, 4, 6,8)	169 GPa	
Poisson Ratio	0.28	0.206
Density	2500 kg m^{-3}	2510 kg m^{-3}
Thermal Expansion Coefficient	$2.5x10^{-6}$ K^{-1}	$7.10x10^{-6}$ K^{-1}
Thermal Conductivity	148 W m^{-1} K^{-1}	1.114 W m^{-1} K^{-1}
Specific Heat	712 J kg^{-1} K^{-1}	858 J kg^{-1} K^{-1}
Electric Conductivity	5.56 mS μm^{-1}	
Stress Gradient	0.6 MPa μm^{-1}	

In this work a (100) silicon wafer is used in the SOIMUMPs fabrication process. Due to the anisotropic nature of single crystalline silicon, the Young's modulus is orientation dependent. The X and Y axes of the MEMS design, shown in figure 1, align with the $\langle 110 \rangle$ silicon crystal directions; therefore the Young's modulus for thermal actuator TA 6 is $E_{[110]}$ = 169 GPa and for TA 5 is $E_{[100]}$ = 130 GPa [28]. Figure 4 compares the displacement behaviours between the thermal actuators TA 5 and TA 6 when the platform is unloaded. Due to the isotropic stress gradient assumption in the SOI layer, the simulated result of the unloaded thermal actuators show a displacement offset due to different Young's moduli used. The actuator TA 5 shows a larger displacement compared to TA 6 since TA 6 has a larger Young's modulus and is therefore stiffer than TA 5. The displacement difference between the two actuators increases with increasing driving power because the effect of the anisotropic Young's modulus dominates at higher thermal expansion force. This is also confirmed through the larger displacement variation of the unloaded platform in figure 2. Figure 5 shows the displacement behaviours between TA 5 and TA 6 when the platform is loaded. In comparison to figure 4, both simulated and experimental results show a reduction in displacement when the gravitation force of the sphere is applied onto the tip of both thermal actuators. In both the experiment and simulation, the vertical displacement of TA 5 is larger than TA 6. In practice, due to different initial (unloaded) deflections, the gravitation force of the sphere is not guaranteed to be equally distributed among the eight thermal actuators, which in turn results in differences between the simulation and experiment. In all the results, this family of electrothermal actuators shows a threshold behaviour which is seen in the simulation and is confirmed in the experiments.

This manuscript is the peer-reviewed, accepted author manuscript of the following article: Blue, R., Li, L., Flockhart, G., & Uttamchandani, D. (2011). MEMS-actuated wavelength drop filter based on microsphere whispering gallery modes. Journal of Micromechanics and Microengineering, 21(11), [115020]. 10.1088/0960-1317/21/11/115020

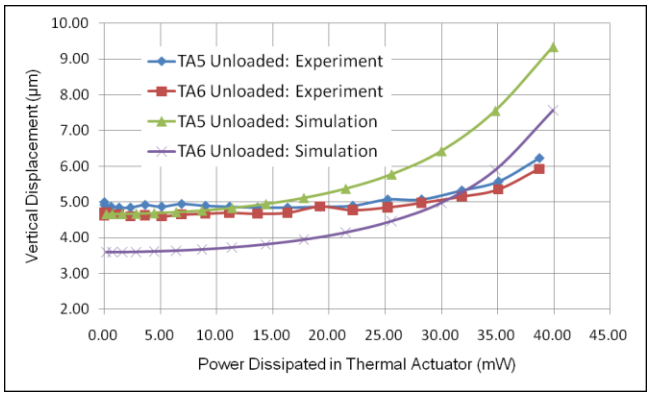

Figure 4. Comparison between the vertical displacements, measured 100 µm from tip, of thermal actuators TA 5 and TA 6 when unloaded.

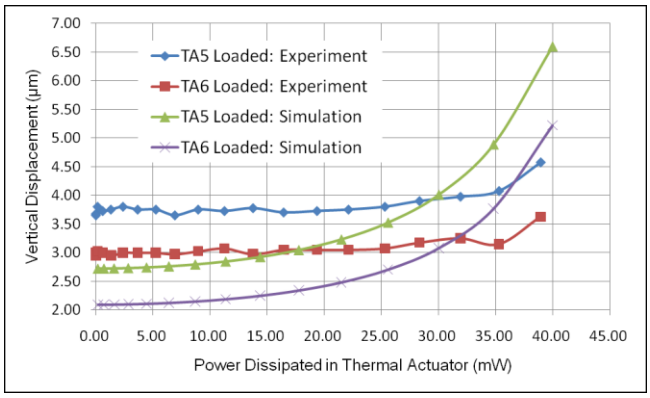

Figure 5. Comparison between the vertical displacements, measured 100 µm from tip, of thermal actuators TA 5 and TA 6 when loaded with a 1.4 mg free sitting sphere.

6. Optical experimental setup

In this work, the optical coupling experiments were performed in two stages. First we investigated the formation of optical tapers suitable for evanescent coupling between the fibre and WGM modes of a spherical resonator. As described in section 1, optical fibre tapers can be used to achieve near lossless coupling to optical microspheres [17]. However to form such tapers, careful control of the taper profile and taper waist dimension is required and this typically requires a computer controlled fabrication system [11,29]. As we did not have access to such a facility, the optical fibre tapers were formed in-house by suspending an uncoated section of single mode optical fibre (SMF-28™) between two arc needle electrodes of a fusion splicer (BFS50, Beale International Technology) and fixing the fibre ends onto two linear translation stages on either side of the splicer, which allowed tension to be applied to the fibre. The taper was formed manually by activating the arc discharge between the electrodes and continually adjusting the translation stages to pull the fibre, thus reducing the diameter of the fibre waist located between the electrodes. By repeated cycles and simultaneous adjustments of arc current and fibre tension, the fibre could be drawn to a fine taper of typically less than 5 µm, see figure 6. The fabricated tapers were adhesive-bonded to a customised glass platform for ease of handling. The insertion losses were measured to

This manuscript is the peer-reviewed, accepted author manuscript of the following article: Blue, R., Li, L., Flockhart, G., & Uttamchandani, D. (2011). MEMS-actuated wavelength drop filter based on microsphere whispering gallery modes. Journal of Micromechanics and Microengineering, 21(11), [115020]. 10.1088/0960-1317/21/11/115020

be 3 to 4 dB on average, although a loss of less than 2 dB could be achieved. The increased loss of these tapers compared to more sophisticated fabrication techniques is primarily due to the poor uniformity of the taper profile and it not being adiabatic [10]. Optical fibre taper losses have been reported as low as 0.04 dB but typically tapers with losses of 0.27 dB can be repeatedly fabricated [11].

To investigate coupling between the fibre taper and a microsphere, an opto-mechanical setup was assembled incorporating the MEMS device, microsphere and micro-positioners to position the optical fibre taper. The glass taper-holder was mounted at an angle of 45° upon a translation stage whose pitch and yaw could be varied. This translation stage was mounted upon a piezoelectric actuated X-Y-Z translation stage controlled by a three-channel piezoelectric driver (17PCS001, Melles Griot) to allow preliminary alignment of the taper with respect to the spherical resonator, see figure 7. Broadband light from an erbium doped fibre amplifier (EDFA) was launched in to an optical fibre and the transmitted power spectrum was measured using an optical spectrum analyser (86140B, Agilent Technologies).

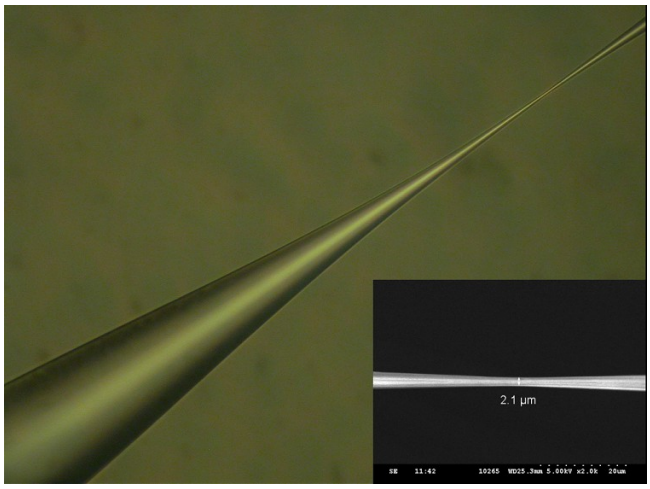

Figure 6. Photograph through a x20 lens of a typical tapered section of an unbroken tapered fibre. The inset shows an SEM image of the fibre waist diameter.

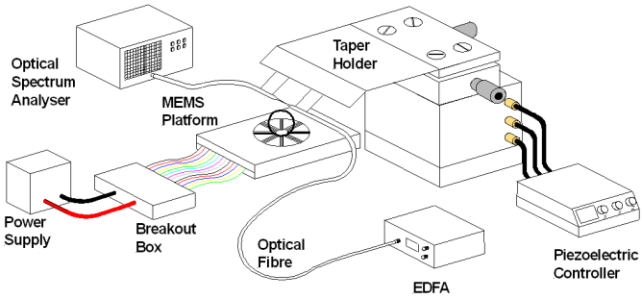

Figure 7. Schematic of the experimental setup showing a microsphere mounted upon a MEMS platform, not to scale.

This manuscript is the peer-reviewed, accepted author manuscript of the following article: Blue, R., Li, L., Flockhart, G., & Uttamchandani, D. (2011). MEMS-actuated wavelength drop filter based on microsphere whispering gallery modes. Journal of Micromechanics and Microengineering, 21(11), [115020]. 10.1088/0960-1317/21/11/115020

The MEMS die was mounted on a custom printed circuit board (PCB) and wire bonded to gold electrodes on the PCB. A 1 mm diameter BK7 sphere (Knight Optical Ltd, UK.) was used as an optical spherical resonator. UV curable adhesive (NOA84, Norland Products Inc.) was placed sparingly at the end of each silicon actuator on the MEMS platform by using a fine needle tip upon an X-Y-Z translation stage and observing the adhesive deposition through a microscope. The sphere was positioned upon the actuator beams and a UV light source was used to cure the adhesive. Figure 8 is a photograph showing the sphere, tapered optical fibre and the MEMS platform. To investigate the effects of having a bonded sphere in a practical device, the displacement of a device was characterised for the case of an unloaded platform, a free sitting 1 mm diameter sphere, and a 1 mm sphere bonded to the actuators.

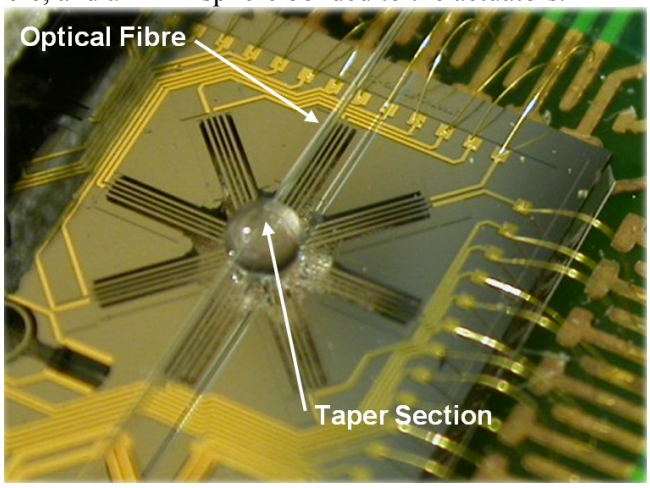

Figure 8. Photograph showing a tapered section of an optical fibre positioned close to apex of BK7 sphere positioned upon the MEMS platform.

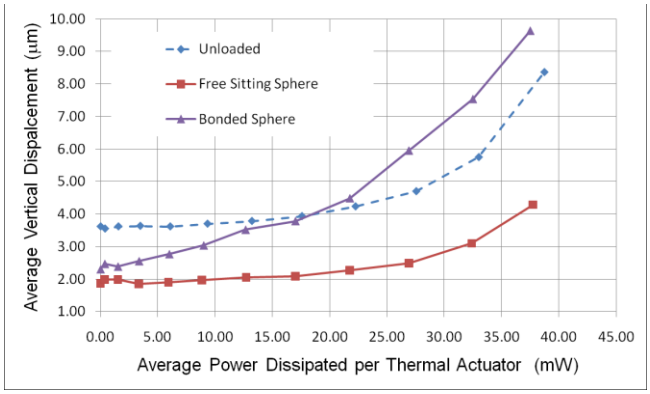

Figure 9. Displacement characterisation of thermal actuators: unloaded (dashed line) and with different loading and UV bonding conditions (solid lines).

Figure 9 shows the average vertical displacement of all the thermal actuators. When the sphere is loaded onto the device and is freely sitting, the device exhibits the same deflection threshold behaviour as the unloaded case but with a vertical offset due to the gravitational force arising from the applied load. However, when the sphere is bonded to all of the thermal actuators of the device, the vertical displacement was observed to be more pronounced at lower drive powers and the total displacement is increased. In the

This manuscript is the peer-reviewed, accepted author manuscript of the following article: Blue, R., Li, L., Flockhart, G., & Uttamchandani, D. (2011). MEMS-actuated wavelength drop filter based on microsphere whispering gallery modes. Journal of Micromechanics and Microengineering, 21(11), [115020]. 10.1088/0960-1317/21/11/115020

cases of the unloaded and free sitting sphere, the thermal expansion of the thermal actuators primarily extends along the longitudinal length of the beams with no obvious vertical displacement. However, once the thermal expansion in the hot beams is constrained by the cold beams, the inner two hot beams buckle and the whole thermal actuator will deform out-of-plane. When the sphere is bonded to all eight thermal actuators, they become mechanically connected through the sphere. Each thermal actuator is no longer constrained at only its base but also at the tip by the sphere connected to the remaining actuators. Bonding the sphere to the MEMS thermal actuator constrains it at both ends which results in out-of-plane deformation for lower differential expansions as the actuator tip is no longer able to freely expand.

To investigate the dynamic response of the device, the vertical displacement of a thermal actuator was characterised when a 5 Hz square wave drive waveform was applied. For a deflection of approximately 1 μm the displacement was observed to achieve a steady state after ~30 ms and ~60 ms for the unloaded case and bonded sphere case respectively.

7. Optical experimental results

The mechanical translation stages were initially used, and the position of the fibre taper was carefully adjusted to within a few microns of the apex of the sphere. The position of the optical taper was then held fixed, and with small adjustments to the electrical drive power to the MEMS actuators, the MEMS platform proved to give very fine control of the coupling of light between the taper and the sphere. With this system a WGM resonance could be established around the circumference of the sphere. Figure 10 shows that by variation of the drive current supplied to the MEMS platform reduced the air gap between the taper and the sphere, leading from partial to full cross coupling when the taper touches the sphere. Here resonances corresponding to both TE and TM modes are visible using light from the unpolarised EDFA source. For a 1 mm BK7 glass sphere of refractive index 1.50071 at 1545 nm, we calculate a free spectral range using equation (1) to be 63.588 GHz, which is equivalent to a wavelength channel separation of 0.51 nm centred at 1545 nm; we experimentally measure a wavelength separation of 0.52 nm in figure 10.

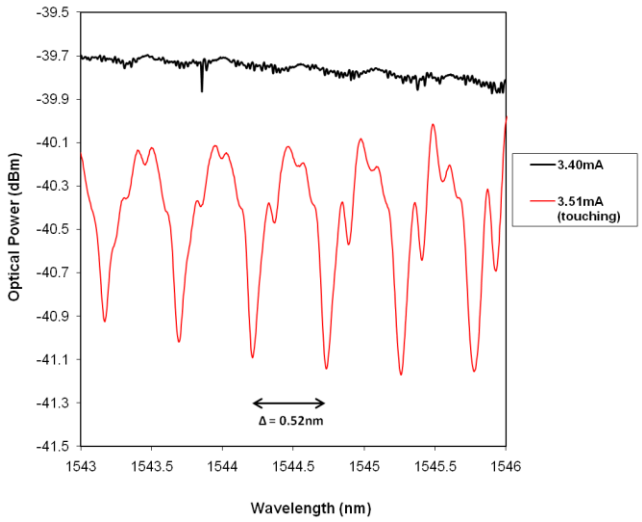

Figure 10. Growth of optical coupling from taper to sphere as air gap decreases with increased current applied to thermal actuators.

The experimental setup was reconfigured to demonstrate active wavelength filtering mediated by the MEMS platform. The EDFA optical source was replaced with an external cavity tuneable diode laser

This manuscript is the peer-reviewed, accepted author manuscript of the following article: Blue, R., Li, L., Flockhart, G., & Uttamchandani, D. (2011). MEMS-actuated wavelength drop filter based on microsphere whispering gallery modes. Journal of Micromechanics and Microengineering, 21(11), [115020]. 10.1088/0960-1317/21/11/115020

(TSL-210, Santec Corporation) and the optical spectrum analyser was replaced with an InGaAs photodiode and amplifier. The laser output was connected to an in-line optical isolator followed by an in-line polariser and a polarisation controller to allow the state of polarisation coupled to the spherical resonator to be optimised. Initially the MEMS device was activated by applying a constant 42 V to the platform, which raised the sphere upwards. The mechanical translation stage supporting the taper was adjusted until a WGM was established. The polarisation controller was adjusted to select either the transverse-electric or transverse-magnetic resonances.

To investigate the repeatability of the coupling between the fibre taper and the spherical resonator, a waveform generator (TGA1242, Thurlby Thandar Instruments Ltd.) was used to generate a sawtooth waveform of frequency 0.05 Hz, which was subsequently amplified by a linear amplifier (P200, FLC Electronics AB), to automatically modulate the drive power to the MEMS platform. The laser was tuned to a wavelength of 1550.4 nm which corresponds to a drop channel. The wavelength was held constant and the transmitted power was measured using the InGaAs photodiode as the MEMs platform was repeatedly cycled from 0 V to 42 V and back to 0 V. Figure 11 shows the applied drive voltage to the MEMS platform and the transmission though the optical fibre as the drive power to the MEMS platform was modulated. This clearly shows the switching on and off of the WGM resonance resulting in the active opto-mechanical induced dropping of the transmission wavelength with a modulation of approximately 0.97 dB.

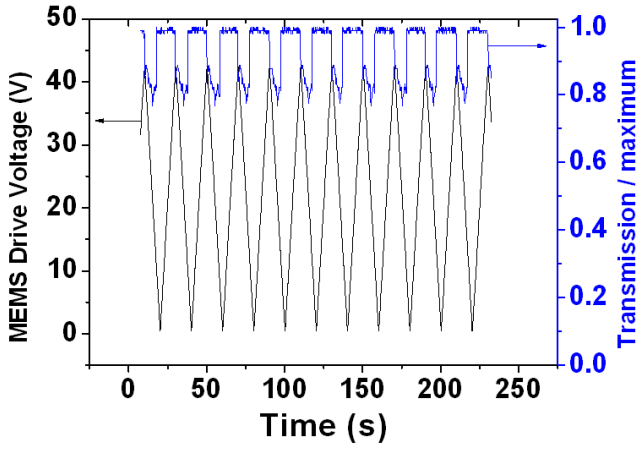

Figure 11. Modulation of light transmission through tapered optical fibre by cycling of MEMS actuators.

8. Discussion

A MEMS platform for controlling the displacement of an optical microsphere relative to a tapered optical fibre was proposed. The design of this platform consisted of eight independent four-beam electrothermal actuators arranged such that their tips form an octagon with an aperture of 800 μm between opposing sides as shown in figure 1. This platform was designed to displace a 1 mm optical sphere placed in the octagon by driving all actuators simultaneously. The thermal distribution and vertical displacement of the actuator beams were simulated using finite element analysis software which indicated a maximum tip displacement of ~13 μm could be achieved at a drive power of 45.4 mW, figure 3(b). After fabrication, the vertical displacement of all 32 beams (4 beams per actuator and 8 actuators) were characterised at an offset of 100 μm from the actuator tip. A standard deviation of approximately ~1 μm was obtained for both the unloaded and loaded case; a potential cause of this is the anisotropic Young's modulus of the silicon. In the

This manuscript is the peer-reviewed, accepted author manuscript of the following article: Blue, R., Li, L., Flockhart, G., & Uttamchandani, D. (2011). MEMS-actuated wavelength drop filter based on microsphere whispering gallery modes. Journal of Micromechanics and Microengineering, 21(11), [115020]. 10.1088/0960-1317/21/11/115020

loaded case, the displacement was observed to decrease by approximately 2 μm which is in excellent agreement with the simulation. The characterisation of the platform was performed with a free-sitting sphere; however this not practical for a real device. The sphere was carefully bonded to the actuators for the optical coupling experiments; therefore the tips of the actuators are effectively coupled together. This may generate additional stress in adjacent actuators resulting in a lateral displacement but due to the spherical nature of the resonator this is not an issue as a circumferential WGM could still be established.

Bonding of the sphere was observed to increase the out-of-plane deflection and we believe it would be interesting to investigate this further in order to optimize the device; however modelling of the hybrid MEMS/sphere structure is non-trivial due to the uncertainties of the material properties of the adhesive and the bonding layer geometry between the actuators and the optical sphere. The fabrication process could result in different volumes of adhesive on each thermal actuator and this could introduce further variations in the observed displacements for each actuator.

We have applied the MEMS platform to control the coupling between an optical spherical resonator and an optical fibre taper. The combination of optical microsphere resonators and tapered optical fibres has been reported previously for potential applications in communications [1]. Also, the optical fibre taper has been reported as the most efficient waveguide to couple to high-Q resonators [17]. In this work we have shown the potential to realise a miniature, low cost, positioning platform that allows tuneable coupling between waveguide and resonator thereby demonstrating the potential to realise controlled switching of selective wavelengths for optical communication devices. We have demonstrated in-line wavelength drop filtering of an optical signal using the MEMS platform to modulate coupling to a WGM in an optical spherical resonator. One of the limiting factors in this proof of concept demonstration is the quality of the optical fibre tapers we were able to produce with our manual setup; however automated fabrication process are available and can repeatedly fabricate high quality, low loss tapers [11,29]. The main disadvantages of the optical fibre taper are its fragility and its limited lifetime due to damage from physical contact with particles and the weakening effect of water vapour ingress in the fused silica. To form a practical system the tapered optical fibre and MEMS platform could be packaged in a dry, clean, hermetically sealed environment. The wavelength selective nature of the device can be tailored by controlling the sphere diameter and refractive index using equation (1). For example, using silica spheres ($n = 1.44427$ at 1529.52 nm) of diameter 1.32 mm and 0.66 mm would result in a free spectral range of 50 GHz and 100 GHz respectively which correspond with the channel separations defined by the ITU grid.

We have investigated the issue of heating from the MEMS actuators on the optical stability of the systems. The dominant effect from heating is likely to be a shift in the resonant wavelengths of the resonator due to thermal expansion of the sphere and a change in refractive index due to the thermo-optic effect. Experimentally, we have not observed large drifts in the resonant wavelengths when the device has been operating due to a build up of heat and the actuator response to a square wave drive voltage achieves a stable displacement after ~60 ms when the sphere is bonded to the actuators. However, we have performed a thermal analysis of the system using a simplified one-dimensional heat conduction approach. We have replaced the sphere with a cylinder of equal diameter and equivalent volume. This results in a change in temperature of the sphere of 7.3 °K for an applied power of 40 mW to each actuator, which induces a shift in optical wavelength of ~0.1 nm. This approach, however, gives a worst case scenario and assumes 100% efficient heat conduction from the MEMS actuator to the sphere and does not consider radiative heating or heat loss through radiation.

Another advantage of the MEMS format described is the potential to include multiple resonators and actuators in a small footprint; thus in-line cascaded optical filters could be realised. This technology could also be applied to compact microsphere lasers where tuning the optical coupling could modulate the laser cavity.

9. Conclusion

This manuscript is the peer-reviewed, accepted author manuscript of the following article: Blue, R., Li, L., Flockhart, G., & Uttamchandani, D. (2011). MEMS-actuated wavelength drop filter based on microsphere whispering gallery modes. Journal of Micromechanics and Microengineering, 21(11), [115020]. 10.1088/0960-1317/21/11/115020

In conclusion, this work reports the first demonstration of tuneable optical coupling between an optical microsphere and tapered optical fibre using a MEMS platform. We have described the design, simulation, experimental characterisation of the device and a proof of concept application by repeatedly switching the coupling for a selected transmitted wavelength. This system could be further optimised by the use of sophisticated fibre taper fabrication equipment and a practical device could be realised with appropriate packaging technologies. Therefore the MEMS system has the potential to develop low insertion loss, compact, switchable, and low cost cascaded filters for telecommunications and other applications using microsphere resonators.

References

[1] Cai M, Hunziker G and Vahala K J 1999 Fiber-optic add-drop device based on a silica microsphere-whispering gallery mode system *IEEE Photonics Technology Letters* **11** 686-7

[2] Barwicz T, Popović M, Rakich P, Watts M, Haus H, Ippen Eand Smith H 2004 Microring-resonator-based add-drop filters in SiN: fabrication and analysis *Optics Express* **12** 1437-42

[3] Dong P, Shafiiha R, Liao S, Liang H, Feng N N, Feng D, Li G, Zheng X, Krishnamoorthy A V and Asghari M 2010 Wavelength-tunable silicon microring modulator *Optics Express* **18** 10941-6

[4] Spillane S M, Kippenberg T J and Vahala K J 2002 Ultralow-threshold Raman laser using a spherical dielectric microcavity *Nature*. **415** 621-3

[5] Arnold S, Khoshsima M, Teraoka I, Holler S and Vollmer F 2003 Shift of whispering-gallery modes in microspheres by protein adsorption *Optics Letters* **28** 272-4

[6] Vollmer F and Arnold S 2008 Whispering-gallery-mode biosensing: label-free detection down to single molecules *Nature Methods* **5** 591-6

[7] Morand A, Zhang Y, Martin B, Phan Huy K, Amans D, Benech P, Verbert J, Hadji E and Fédéli J M 2006 Ultra-compact microdisk resonator filters on SOI substrate *Optics Express* **14** 12814-21

[8] Serpenguzel A, Arnold S and Griffel G 1995 Excitation of resonances of microspheres on an optical fiber *Optics Letters* **20** 654-6

[9] Ilchenko V S, Yao X S and Maleki L 1999 Pigtailing the high-Q microsphere cavity: a simple fiber coupler for optical whispering-gallery modes *Optics Letters* **24** 723-5

[10] Knight J C, Cheung G, Jacques F and Birks T A 1997 Phase-matched excitation of whispering-gallery-mode resonances by a fiber taper *Optics Letters* **22** 1129-31

[11] Ding L, Belacel C, Ducci S, Leo G and Favero I 2010 Ultralow loss single-mode silica tapers manufactured by a microheater *Applied Optics* **49** 2441-5

[12] Carmon T, Wang S Y T, Ostby E P and Vahala K J 2007 Wavelength-independent coupler from fiber to an on-chip cavity, demonstrated over an 850nm span *Optics Express* **15** 7677-81

[13] Braginsky V B, Gorodetsky M L and Ilchenko V S 1989 Quality-factor and nonlinear properties of optical whispering-gallery modes *Physics Letters A* **137** 393-7

[14] Bilici T, Isci S, Kurt A and Serpenguzel A 2004 Microsphere-Based Channel Dropping Filter With an Integrated Photodetector *IEEE Photonics Technology Letters***16** 476-8

[15] Lee M C M and Wu M C 2006 Tunable coupling regimes of silicon microdisk resonators using MEMS actuators *Optics Express* **14** 4703-12

[16] Takahashi K, Kanamori Y, Kokubun Y and Hane K 2008 A wavelength-selective add-drop switch using silicon microring resonator with a submicron-comb electrostatic actuator *Optics Express* **16** 14421-8

This manuscript is the peer-reviewed, accepted author manuscript of the following article: Blue, R., Li, L., Flockhart, G., & Uttamchandani, D. (2011). MEMS-actuated wavelength drop filter based on microsphere whispering gallery modes. Journal of Micromechanics and Microengineering, 21(11), [115020]. 10.1088/0960-1317/21/11/115020

[17] Spillane S M, Kippenberg T J, Painter O J and Vahala K J 2003 Ideality in a Fiber-Taper-Coupled Microresonator System for Application to Cavity Quantum Electrodynamics *Physical Review Letters* **91** 043902
[18] Collot L, Lefèvre-Seguin V, Brune M, Raimond J M and Haroche S 1993 Very High- Q Whispering-Gallery Mode Resonances Observed on Fused Silica Microspheres *Europhysics Letters (EPL)* **23** 327-34
[19] Chiasera A, Dumeige Y, Féron P, Ferrari M, Jestin Y, Nunzi Conti G, Pelli S, Soria S and Righini G C 2010 Spherical whispering-gallery-mode microresonators *Laser & Photonics Reviews* **4** 457-82
[20] Laine J P, Little B E, Lim D R, Tapalian H C, Kimerling L C and H.A. Haus 2000 Planar integrated wavelength-drop device based on pedestal antiresonant reflecting waveguides and high-Q silica microspheres *Optics Letters* **25** 1636-8
[21] Cai M, Painter O and Vahala K J 2000 Observation of Critical Coupling in a Fiber Taper to a Silica-Microsphere Whispering-Gallery Mode System *Physical Review Letters* **85** 74-7
[22] Fujita H 1998 Micro actuators and their applications *Microelectronics Journal* **29** 637-40
[23] Li L, Brown J G and Uttamchandani D 2002 Study of scratch drive actuator force characteristics *Journal of Micromechanics and Microengineering* **12** 736-41
[24] Park J S, Chu L L, Oliver A D and Gianchandani Y B 2001 Bent-beam electrothermal actuators-Part II: Linear and rotary microengines *Journal of Microelectromechanical Systems* **10** 255-62
[25] http://www.memscap.com/en_mumps.html, "SOIMUMPS Multi-User Process," *MEMSCAP Inc.*
[26] Miller D C, Boyce B L, Dugger M T, Buchheit T E and Gall K 2007 Characteristics of a commercially available silicon-on-insulator MEMS material *Sensors and Actuators A: Physical*, **138** 130-144
[27] Cho C H 2009 Characterization of Young's modulus of silicon versus temperature using a 'beam deflection' method with a four-point bending fixture *Current Applied Physics* **9** 538-45
[28] Hopcroft M A, Nix W D and Kenny T W 2010 What is the Young's Modulus of Silicon? *Journal of Microelectromechanical Systems* **19** 229-38
[29] Dimmick T E, Kakarantzas G, Birks T A and Russell P S J 1999 Carbon Dioxide Laser Fabrication of Fused-Fiber Couplers and Tapers *Applied Optics* **38** 6845-8

This manuscript is the peer-reviewed, accepted author manuscript of the following article: Blue, R., Li, L., Flockhart, G., & Uttamchandani, D. (2011). MEMS-actuated wavelength drop filter based on microsphere whispering gallery modes. Journal of Micromechanics and Microengineering, 21(11), [115020]. 10.1088/0960-1317/21/11/115020